Nitroxides Block DNA Scission and Protect Cells from Oxidative Damage

Amram Samuni,*,‡ Dina Godinger,‡ Jacob Aronovitch,‡ Angelo Russo,§ and James B. Mitchell§

Molecular Biology, School of Medicine, Hebrew University, Jerusalem 91010, Israel, and Radiation Oncology Branch, Clinical Oncology Program, Division of Cancer Treatment, National Cancer Institute, National Institutes of Health, Bethesda, Maryland 20892

Received April 11, 1990; Revised Manuscript Received September 11, 1990

ABSTRACT: The protective effect of cyclic stable nitroxide free radicals, having SOD-like activity, against oxidative damage was studied by using *Escherichia coli xthA* DNA repair-deficient mutant hypersensitive to H_2O_2. Oxidative damage induced by H_2O_2 was assayed by monitoring cell survival. The metal chelator 1,10-phenanthroline (OP), which readily intercalates into DNA, potentiated the H_2O_2-induced damage. The extent of in vivo DNA scission and degradation was studied and compared with the loss of cell viability. The extent of DNA breakage correlated with cell killing, supporting previous suggestions that DNA is the crucial cellular target of H_2O_2 cytotoxicity. The *xthA* cells were protected by catalase but not by superoxide dismutase (SOD). Both five- and six-membered ring nitroxides, having SOD-like activity, protected growing and resting cells from H_2O_2 toxicity, without lowering H_2O_2 concentration. To check whether nitroxides protect against $O_2^{\cdot-}$-independent injury also, experiments were repeated under hypoxia. These nitroxides also protected hypoxic cells against H_2O_2, suggesting alternative modes of protection. Since nitroxides were found to reoxidize DNA-bound iron(II), the present results suggest that nitroxides protect by oxidizing reduced transition metals, thus interfering with the Fenton reaction.

The goal of protecting biological systems from oxidative damage involves several lines of research, including (a) elevation of intra- and extracellular levels of enzymes that detoxify deleterious oxygen-derived species, (b) synthesis of cell-permeable compounds that mimic the activities of such enzymes, (c) identification of compounds that may protect by scavenging $^{\cdot}OH$ radicals, and (d) use of chelating agents capable of modifying the activity of redox-active transition metals or altering their specific binding to crucial cellular targets.

Stable nitroxide free radicals are widely used in biophysical studies and have previously been reported to react with various free radicals (Khloplyankina et al., 1965; Brownlie & Ingold, 1967; Robbins & Eastman, 1970; Rigo et al., 1977; Mehlhorn & Packer, 1984; Belkin et al., 1987). Superoxide radicals ($O_2^{\cdot-}$) were found to reduce the five-membered ring nitroxide 2-ethyl-2,5,5-trimethyl-3-oxazolidineoxyl (OXANO)[1] to its corresponding hydroxylamine, 2-ethyl-1-hydroxy-2,5,5-trimethyl-3-oxazolidine (OXANOH) (Samuni et al., 1989):

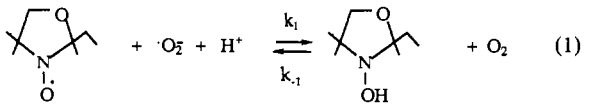

(1)

In addition, OXANOH itself is capable of reducing $O_2^{\cdot-}$ to H_2O_2 (Rosen et al., 1982):

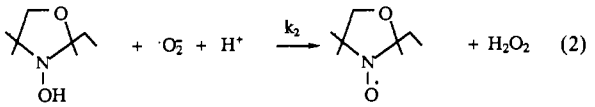

(2)

Adding equations 1 and 2 yields a net dismutation reaction, thus, under a continuous flux of $O_2^{\cdot-}$, the OXANO/OXANOH redox couple achieves a steady-state distribution and as a result of converting $O_2^{\cdot-}$ into H_2O_2 and O_2 mimics the activity of superoxide dismutase (SOD) (Samuni et al., 1988):

$$2H^+ + 2O_2^{\cdot-} \rightarrow H_2O_2 + O_2 \quad (3)$$

The low cytotoxicity, relative stability, solubility in both lipophilic and hydrophilic compartments, and low reactivity toward oxygen and H_2O_2 make OXANO/OXANOH a metal-independent SOD mimic superior to other low-molecular weight metal-based SOD mimics that rapidly react with O_2 and tend to dissociate in vivo (Darr et al., 1987). Recently, several other five- as well as six-membered ring nitroxides free radicals were found to possess SOD-mimetic activity (Samuni et al., 1990). The present study includes OXANO, the more lipophilic derivative spiro[cyclohexane-1,2′-doxyl] (CHDO), and the six-membered cyclic nitroxides TEMPO, TEMPOL, and TEMPAMIN.

Since low molecular weight nitroxides can readily enter the cell, they would be expected to afford better protection against intracellular damage than exogenously added SOD, which because of size may be restricted from entry into the cell. To test the extent and nature of the presumed in vivo protective effect of nitroxides against oxidative injury, specific H_2O_2-mediated cell killing and DNA scission were studied. The *Escherichia coli* mutant *xthA*, which is deficient in exonuclease III and is known to be hypersensitive to H_2O_2 (Demple et al., 1983; Imlay & Linn, 1986; Linn & Imlay, 1987; Denq & Fridovich, 1989), was selected as a sensitive test system. The cleavage of DNA and loss of viability of growing or resting cells were investigated together with the nitroxides' protective effects. The results indicated that (a) DNA is the critical site of damage in growing cells, (b) both hydrophilic and lipophilic nitroxides prevent DNA injury and cell killing, and (c) protection from H_2O_2-induced damage involves also $O_2^{\cdot-}$-independent reactions, most probably reoxidation of reduced metal.

‡ Hebrew University.
§ National Institutes of Health.

[1] Abbreviations: EPR, electron paramagnetic resonance; TEMPO, 2,2,6,6-tetramethylpiperidine-1-oxyl; TEMPOL, 4-hydroxy-2,2,6,6-tetramethylpiperidine-1-oxyl; TEMPAMIN, 4-amino-2,2,6,6-tetramethylpiperidineoxyl; OXANO, 2-ethyl-2,5,5-trimethyl-3-oxazolidineoxyl; OXANOH, 2-ethyl-1-hydroxy-2,5,5-trimethyl-3-oxazolidine; CHDO, spiro[cyclohexane-1,2′-doxyl] (spiro[cyclohexane-1,2′-5′,5′-dimethyl-3′-oxazolidineoxyl]); CrOx, tris(oxalato)chromate(III); OP, 1,10-phenanthroline; EDTA, ethylenediaminetetraacetate; SOD, superoxide dismutase; CAT, catalase; DFO, desferrioxamine; ssb, single-stranded breaks; dsb, double-stranded breaks.

0006-2960/91/0430-555$02.50/0

Experimental Procedures

Materials. Desferrioxamine (Desferal) was a gift from Ciba Geigy; superoxide dismutase and 1,10-phenanthroline were obtained from Sigma; $FeSO_4 \cdot 7H_2O$ was obtained from Mallinckrodt; 3,3-dimethyl-1-oxa-4-azaspiro[4.5]dec-4-yloxy, free radical (spiro[cyclohexane-1,2′-doxyl]) (CHDO), 2,2,6,6-tetramethylpiperidine-1-oxyl (TEMPO), 4-hydroxy-2,2,6,6-tetramethylpiperidine-1-oxyl (TEMPOL), and 4-amino-2,2,6,6-tetramethylpiperidineoxyl (TEMPAMIN) were obtained from Aldrich; H_2O_2 was obtained from Merck; tris(oxalato)chromate(III) (CrOx), $K_3[Cr(C_2O_4)_3] \cdot 3H_2O$, was prepared as described (Bailar & Young, 1939) for use as a paramagnetic broadening agent (Lai et al., 1988). All other chemicals were prepared and used without further purification. Distilled deionized water was used throughout.

Synthesis of OXANO. The synthesis of 2-ethyl-2,5,5-trimethyl-3-oxazolidineoxyl (OXANO) was performed as previously described (Keana et al., 1967). Briefly, to produce the amine, 2-butanol was reacted with 2-amino-2-methyl-2-propanol in benzene by using *p*-toluenesulfonic acid catalysis. The formation of the cyclic structure resulted in the elimination of water. The volume of water collected in a Dean Stark apparatus was monitored and used to gauge the reaction progress. The amine thus produced was purified through fractional distillation under reduced pressure, characterized by means of NMR, IR, UV, and mass spectroscopy, oxidized to the nitroxide by using *m*-chloroperbenzoic acid, and purified by silica flash chromatography. Octanol/water partition ratios were determined by shaking for 15 min the nitroxide with octanol and water within a separatory funnel. The system was allowed to equilibrate, aliquots were taken from both phases, and the nitroxide distribution was determined by comparing the intensities of the respective nitroxide EPR signal under N_2.

Culture Preparation and H_2O_2 Treatment of Cells. E. coli KL-16 and its *xthA* mutant were grown at 37 °C in glucose–mineral medium supplemented with 1% casamino acids. Log phase cells in growth medium or washed cells in pH 7.4 1 mM phosphate buffer containing 1 mM $MgSO_4$ were treated for varying periods of time with H_2O_2 (0.1–5 mM) in the absence or presence of OP. The reactions were terminated by adding 130 units/mL catalase (CAT) and 20 μM EDTA, and the treated cells were plated on L-agar. The agar plates were incubated overnight at 37 °C and subsequently colonies were counted.

Assay of Intracellular DNA Breakage. The DNA of treated cells were purified by conventional methods (Maniatis et al., 1982). Briefly, following varying periods of treatment, samples containing 3×10^8 *E. coli xthA* cells were collected by centrifugation, resuspended in Tris–EDTA buffer, pH 7.6, incubated with lysozyme (0.2 mg/mL, 4 °C, 30 min) followed by proteinase K (50 μg/mL, 37 °C, 1 h), and mixed gently 1:1 with chloroform/isoamyl alcohol (24:1). The aqueous phase that contained the DNA was separated from the proteins by three successive centrifugations (10000 rpm, 5 min) each followed by additions of the chloroform/isoamyl alcohol. The aqueous phase containing the DNA was removed, made 0.1 M in NaCl, mixed with 2 volumes of cold ethanol, kept 24 h at −20 °C, and then centrifuged (15000 rpm, 0 °C, 10 min). The supernatant was discarded, the pellet was dried and suspended in 0.2 M Tris–EDTA, pH 7.6, and RNAse was added (50 μg/mL, 37 °C, 1 h) to remove RNA. To assay for double-strand breaks (dsb), samples of 1 μg of the isolated bacterial DNA were applied to horizontal, 0.6–1% agarose, slab gels in pH 8 Tris–acetate ETA buffer containing 0.5 μg/mL ethidium bromide and electrophoresed at a potential gradient of 2.5 V/cm. To assay for single-strand breaks (ssb), the DNA was incubated at pH 12 for 10 min, neutralized, and then electrophoresed. Following electrophoresis the gels were illuminated with UV light and photographed by using 665 Polaroid positive–negative film.

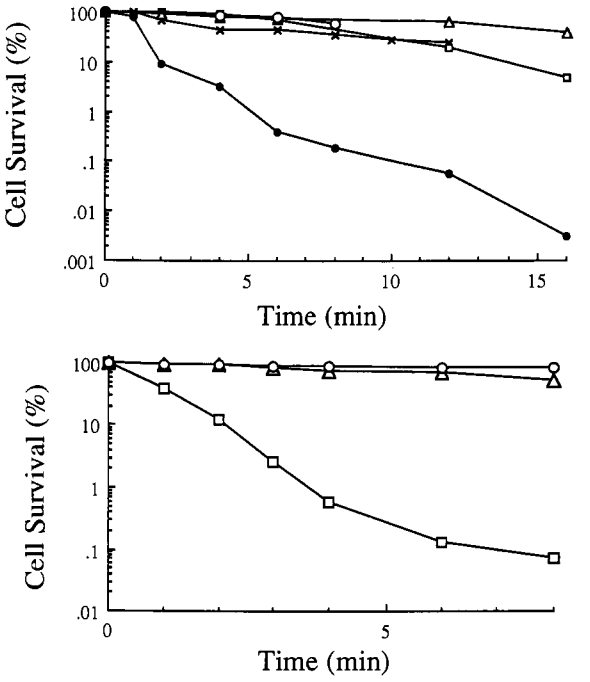

FIGURE 1: (a, Top) The effect of nitroxides of H_2O_2-induced killing of growing *E. coli xthA* cells. The surviving fraction of 5×10^7 cells/mL following incubation at 37 °C in growth medium with 5 mM H_2O_2 in the absence (solid symbols) and presence (open symbols) of 5 mM nitroxide: TEMPO (○), TEMPAMIN (×), OXANO (△), or CHDO (□). (b, Bottom) OXANO protects against 1,10-phenanthroline-catalyzed killing of resting *E. coli xthA* cells exposed to H_2O_2. Time dependence of cell surviving fraction following exposure of resting cells in phosphate buffer at 37 °C to 0.5 mM H_2O_2 (circles) without OP, (squares) with 20 μM OP, and (triangles) with 20 μM OP + 5 mM OXANO.

Electron Paramagnetic Resonance (EPR) Measurements. Samples were drawn by a syringe into a gas-permeable, 0.8-mm inner diameter, Teflon capillary. Each capillary was inserted into a quartz EPR tube and then horizontally placed within the EPR cavity. Air or N_2 was flowed around the sample within the spectrometer cavity, and the EPR spectra were recorded on a Varian E9 or E4 X-band spectrometer, with a field set at 3357 G, modulation frequency of 100 KHz, modulation amplitude of 1 G, and nonsaturating microwave power. The EPR spectrometer was interfaced to an IBM PC and the spectra and kinetic curves were down-loaded to the computer.

Results

H_2O_2 Effect on Cell Survival. Incubation of log phase dividing *xthA* cells (5×10^7 cells/mL) in growth medium containing 5 mM H_2O_2 for various periods of time resulted in extensive loss of colony-forming ability (Figure 1a). Washed resting *xthA* cells suspended in buffer were previously found relatively stable and only slightly more sensitive to H_2O_2 than the wild-type parent strain (Aronovitch et al., 1986a), thus indicating that active cellular metabolism is required for H_2O_2-mediated damage (Aronovitch et al., 1986a). The present experiments showed that cells growing on glucose-supplemented medium have a low endogenous CAT content; therefore, the initial $[H_2O_2]$ introduced decreased by only about 20% during the experiment, as measured by a modification of the ferrithiocyanate method (Thurman et al., 1972), both in the absence and presence of nitroxide. SOD (50

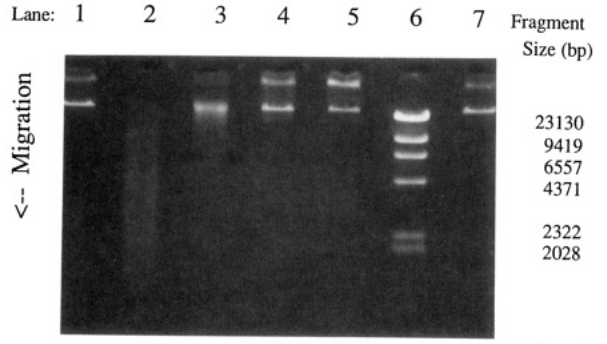

FIGURE 2: TEMPOL blocks in vivo DNA ssb and dsb induced by H_2O_2. *E. coli xthA*, 3×10^7 cells/mL, in 5 mM MES buffer, pH 6.5 at 37 °C, was exposed for 6 min to 1 mM H_2O_2 with or without TEMPOL. The reaction was terminated by 130 units/mL CAT. The cells were sampled and plated for clonogenic assay. Concurrently, the bacterial DNA was isolated and electrophoresed for scission analysis. Lanes 1–7 in the electrophoregram represent the migration profiles of DNA isolated from cells following different treatments. Lanes 1–3 ssb: (1) control ($-H_2O_2$); (2) $+H_2O_2$; (3) H_2O_2 + 10 mM TEMPOL. Lanes 4–7 dsb: (4) $+H_2O_2$; (5) H_2O_2 + 10 mM TEMPOL; (6) molecular weight markers, *Hin*dIII digest of λ-DNA, fragment sizes are noted; (7) control ($-H_2O_2$).

units/mL) had no protective effect, unlike 50 units/mL CAT that fully protected the cells (data not shown). OXANO (5 mM), however, protected the cells (Figure 1a). The experiment was repeated using CHDO (the five-membered ring nitroxide, spiro[cyclohexane-1,2′-doxyl), which is similar to OXANO dismutates $O_2^{\bullet-}$ but is more hydrophobic than OXANO as demonstrated by their octanol/water partition ratios, 80.4 and 9.9, respectively. CHDO would, therefore, be expected to accumulate to a greater extent in membrane compartments; nevertheless, it protected the cells from H_2O_2 cytotoxicity as seen in Figure 1a. Similar protection was provided by the six-membered cyclic nitoxides TEMPO, TEMPOL, and TEMPAMIN (Figure 1a).

Effect of 1,10-Phenanthroline (OP). Endogenous transition metals were previously reported to potentiate H_2O_2 toxicity in growing *xthA E. coli* cells (Aronovitch et al., 1986a). This cytotoxicity could be extended to resting cells by adding OP, which avidly binds copper and iron and interchelates into DNA. OP exerts "site-specific" damage, dramatically potentiates DNA cleavage (Thederahn et al., 1989), and can help in elucidating the critical sites of cell injury and the role of intracellular transition metals. Previous studies demonstrated that lower concentrations of H_2O_2 are required to cause DNA cleavage and cell killing in the presence of OP than in its absence (Aronovitch et al., 1986a). The present results showed that in the presence of 20 μM OP resting cells also were killed by H_2O_2 and that the nitroxides tested also protected the cells against OP + H_2O_2. In the absence of hydrogen peroxide, 20 μM OP did not affect cell survival. Typical survival curves obtained in the absence and presence of OXANO are demonstrated in Figure 1b.

In Vivo DNA Cleavage. The DNA of the *xthA* cells is, most likely, the critical target of the H_2O_2 effect. To examine this possibility, dividing *xthA E. coli* cells were exposed in growth medium at 37 °C to 1 mM H_2O_2, the reaction was terminated after varying periods of time by 130 units/mL CAT and 0.5 mM EDTA, the bacterial DNA was isolated and electrophoresed on agarose slab gels, and the extents of ssb and dsb were studied. Simultaneously, the cells were also sampled and cell survival was assayed clonogenically. A typical electrophoregram is illustrated in Figure 2 where the migration profiles of the bacterial DNA (1 μg per lane) reflect the various degrees of DNA fragmentation. The migration profile observed in lane 2 demonstrates DNA fragments of predominantly 10^2–(2×10^4) base pairs, as judged by comparison to the endonuclease *Hin*dIII digest of λ-DNA (lane 6), reflecting extensive ss DNA breakage. Comparing, however, lane 4 and lane 2 indicates only marginal ds breakage. Lanes 3 and 5 demonstrate the protective effect of TEMPOL against DNA scission. This effect of TEMPOL was mainfested also in cell survival. The surviving fraction of cells treated with H_2O_2 in the absence of TEMPOL (corresponding to lanes 2 and 4) decreased to 17%. Conversely, cells treated in the presence of TEMPOL (corresonding to lanes 3 and 5) maintained 100% survival.

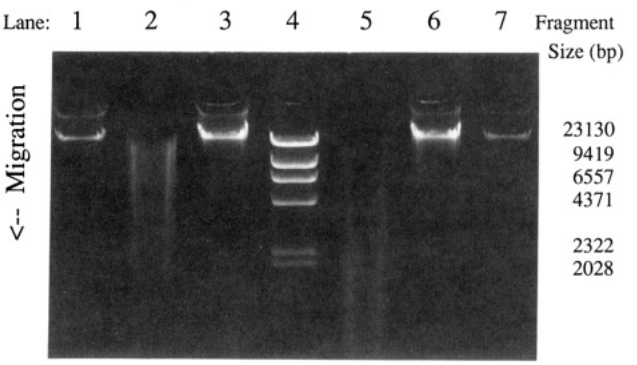

FIGURE 3: TEMPOL blocks in vivo DNA dsb induced by OP + H_2O_2. *E. coli xthA*, 3×10^7 cells/mL, in 5 mM MES buffer, pH 6.5 at 37 °C, was exposed for various periods of time to 20 μM OP + 1 mM H_2O_2 with or without 10 mM TEMPOL. The reaction was terminated by 130 units/mL CAT. The cells were sampled and plated for viability assay, and the bacterial DNA was isolated and electrophoresed for scission analysis. (a, Top) Electrophoregram representing the extent of dsb of DNA isolated from cells following different treatments: (1) control ($-H_2O_2$); (2) 2-min exposure; (3) 2-min exposure, +TEMPOL; (4) molecular weight markers, *Hin*dIII digest of λ-DNA, fragment sizes are noted; (5) 4-min exposure; (6) 4-min exposure, +TEMPOL; (7) control ($-H_2O_2$, +TEMPOL). (b, Bottom) Respective survival of cells corresponding to lanes 1–3, 5, and 6.

DNA Scission in the Presence of OP. Figure 3 demonstrates the results of a similar set of experiments carried out in the presence of 20 μM OP that intercalates into DNA and potentiates H_2O_2 injury. In the presence of 20 μM OP, a shorter exposure of the cells to lower H_2O_2 concentration was sufficient to cause a large number of dsb as seen in Figure 3a, lanes 2 and 5. The respective effect on cell survival is presented in Figure 3b. OP-potentiated degradation of the bacterial DNA and the killing of the cells were prevented by 10 mM TEMPOL (lanes 3 and 6) and TEMPO (data not shown).

Anoxic H_2O_2-Induced Damage. Assuming that nitroxides protect by their SOD-like activity implies that in the absence of $O_2^{\bullet-}$ the nitroxide would fail to protect. To check this assumption the effect of nitroxides under anoxia has been investigated. The rate of killing of growing *xthA E. coli* cells exposed in growth medium to 5 mM H_2O_2 under anoxic conditions is greater than that inflicted under air, as previously reported (Aronovitch et al., 1986a) and as seen in Figure 4. To check whether nitroxides provide protection in the absence of oxygen also, *xthA* cells suspended in growth medium were

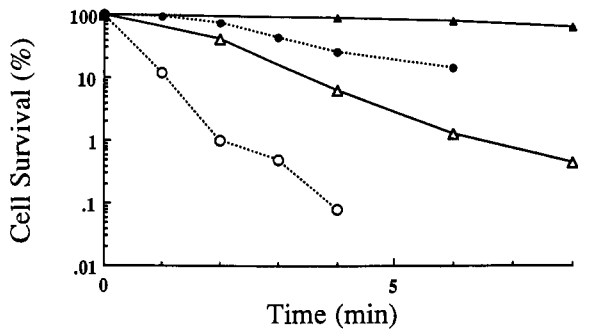

FIGURE 4: TEMPOL protects aerobic and hypoxic *E. coli xthA* cells against H_2O_2-induced killing. Time dependence of cell surviving fraction following incubation of 5 mM H_2O_2 with 5×10^7 cells/mL in growth medium at 37 °C under hypoxic (circles) or aerobic conditions (triangles) in the absence (open symbols) or presence (closed symbols) of 5 mM TEMPOL.

bubbled with nitrogen 20 min before and during exposure to 5 mM H_2O_2. Figure 4 shows that 5 mM TEMPOL greatly lowered the rate of cell killing. Similar results were obtained with 10 mM CHDO, which reduced the rate of killing about 3-fold (data not shown).

Nitroxide Localization. Figure 5 illustrates the nitroxides EPR spectra of 1 mM nitroxide recorded in the presence of 1.4×10^{10} *E. coli* cells/mL. The EPR signals of OXANO (trace a) and CHDO (trace c) represent the total concentration of intra- and extracellular spin label. Tris(oxalato)chromate (CrOx) is a paramagnetic broadening agent that is excluded from the intracellular volume space and causes the EPR signal from extracellular species to become nondetectable (Lai et al., 1988). When the nitroxides were incubated with 110 mM CrOx their EPR signal became undetectable. Upon the addition of the cells, however, a fraction (about 2%) of the original signal was restored. The lesser signal corresponds to the fractional volume occupied by the cells in the examined sample, reflecting the distribution of the nitroxide between the intra- and extracellular compartments. The observable line broadening of the intracellular signal of CHDO indicates a significantly decreased freedom of motion (anisotropy) of the intracellular nitroxide, suggesting that CHDO, though not

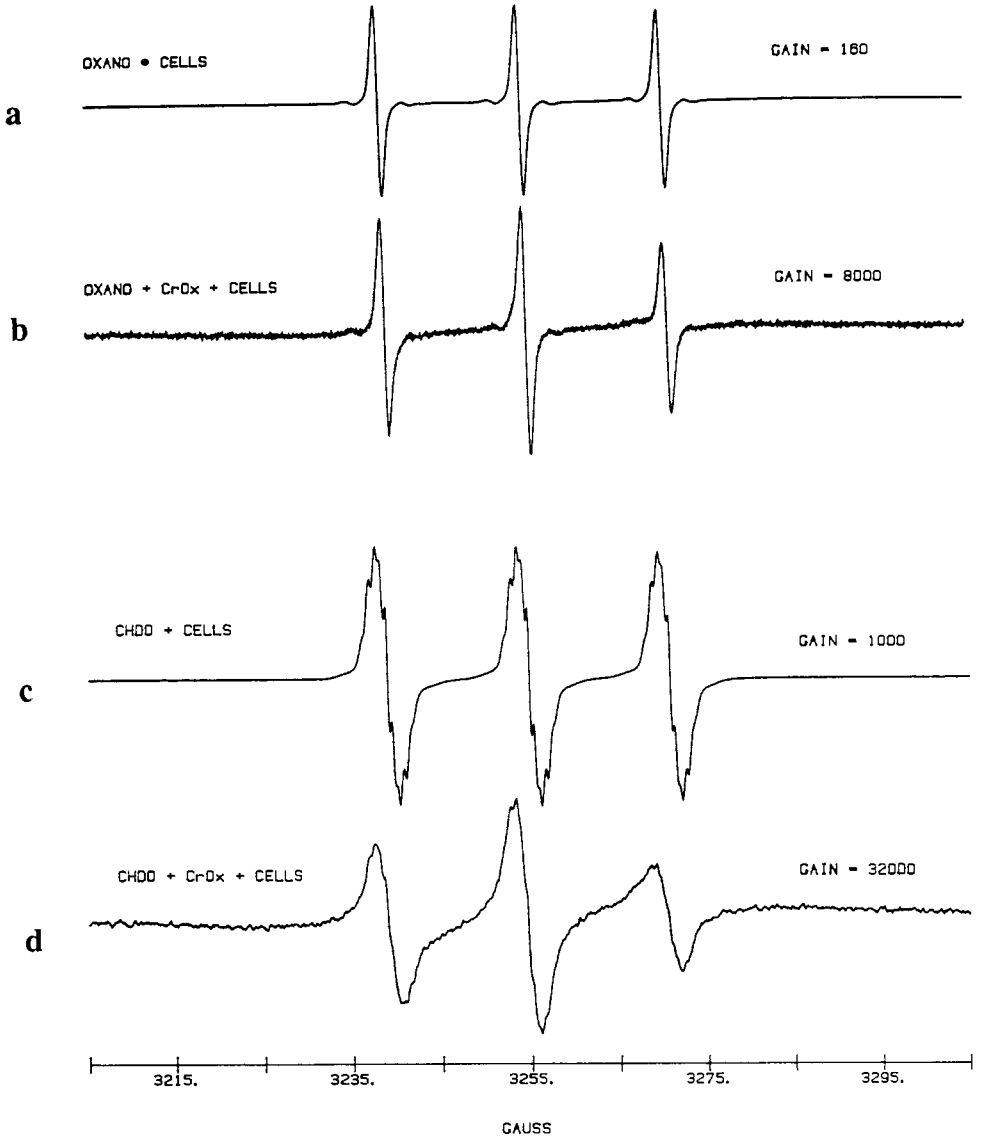

FIGURE 5: Nitroxide partition inside and outside the cell. EPR spectrum of OXANO (traces a and b) and CHDO (traces c and d) demonstrating the partitioning of the nitroxide in both the intra- and extracellular space of *E. coli* cells: The EPR signal intensity of the total concentration of the nitroxide (intra- and extracellular) in 1.4×10^{10} cells/mL was measured in the absence (traces a and c) and the presence (traces b and d) of 110 mM CrOx, an extracellular paramagnetic broadening agent. The spectra shown in traces b and d, revealing the intracellular nitroxide exclusively, were recorded approximately 30 s after adding the cells to the nitroxide in the presence of CrOx. The background EPR signal of CrOx was measured separately and subtracted from the other spectra.

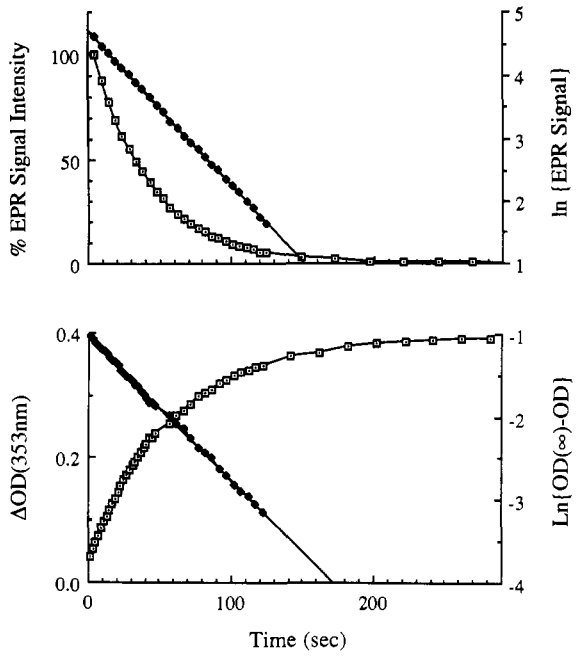

FIGURE 6: Reaction between OXANO and DNA–Fe(II). OXANO was anoxically mixed with iron(II) in 50 mM MOPS buffer, pH 7.0, containing 0.1 mg/mL salmon DNA at 22 °C. The appearance of DNA–Fe(III) was spectrophotometrically monitored at 353 nm, whereas the spin loss of OXANO was monitored by following its EPR signal. Top: Time dependence of ΔOD_{353nm} (open symbols) and of ln ($OD_\infty - OD_t$) (solid symbols) resulting upon mixing 1 mM OXANO with 0.1 mM Fe(II). Bottom: Time dependence of EPR signal (open symbols) and ln (EPR signal) (solid symbols) upon mixing 50 μM OXANO with 1 mM Fe(II).

OXANO, is located primarily in a membranous compartment.

The Reaction between Iron(II) and Nitroxides. The protection against H_2O_2 toxicity of hypoxic cells suggested an alternative mode of nitroxide action, independent of $O_2^{\bullet-}$ dismutation. One possible mechanism might be through reaction with intracellular redox-active metals. To study such a possibility, iron(II) was anoxically mixed with OXANO in the presence of 0.1 mg/mL salmon DNA. Consequently, the iron has been oxidized to Fe(III) and the EPR signal of the nitroxide disappeared. The reaction kinetics were investigated by maintaining either OXANO or Fe(II) in excess and monitoring the absorbance due to DNA–Fe(III) (Figure 6, top) and the nitroxide spin loss (Figure 6, bottom). Both the decay of the EPR signal and the appearance of OD_{353nm} obeyed pseudo-first-order kinetics from which the second-order reaction rate constant was calculated as 24 or 17 M^{-1} s^{-1} by using the data of EPR of spectra absorbance, respectively. When CHDO was anoxically mixed with DNA–Fe(II), a similar reaction took place having a second-order reaction rate constant of 30 M^{-1} s^{-1}.

Discussion

All the nitroxides tested in the present study possess SOD-mimetic activity in vitro (Samuni et al., 1990), rapidly partition into the cells (Figure 5), and exert extensive cytoprotection against H_2O_2 (Mitchell et al., 1990). Although CHDO accumulates predominantly in membranous cellular compartments (Figure 5), both TEMPOL and CHDO show comparable protective effects (Figure 1a) and similar partition between the intra- and extracellular compartments (Figure 5), despite the very large difference in their hydrophobicity. However, the hypoxic cytoprotection afforded by nitroxides suggests an interference with superoxide-independent cell injury. The present results do not exclude the possibility that nitroxide can protect against $O_2^{\bullet-}$-mediated damage, but they indicate that other modes of action are also operative. Lacking a functional exonuclease III, *xthA* is 30-fold more susceptible than wild-type *E. coli* to killing by H_2O_2 (Demple et al., 1983; Aronovitch et al., 1986a). This mutant is, therefore, particularly suitable for the study of protection against intracellular DNA damage. When suspended in buffer, however, *xthA* cells do not differ from the wild-type cells in their susceptibility to H_2O_2-induced damage. This suggests that active cellular metabolism is a prerequisite for cell injury (Aronovitch et al., 1986a; Imlay & Linn, 1986). In addition, previous studies showed that preincubation of the cells with desferrioxamine (DFO) decreased the rate of cell killing (Aronovitch et al., 1986b), indicating that intracellular transition-metal ions, most likely iron, participate in H_2O_2-induced damage to *xthA* cells. The well-recognized importance of transition metals in H_2O_2-induced cytotoxicity (Sagripanti & Kraemer, 1989) is also illustrated by the enhanced cytotoxicity occurring in the presence of OP as seen in Figures 1b and 3. The commonly proposed mechanism to account for the metal-catalyzed H_2O_2-induced damage invokes the redox reactions of transition-metal ions (Goldstein & Czapski, 1986). It is possible that only a trace fraction of the total cellular iron and copper is "redox-active" in a way that can lead to biological damage. Yet, neither the level nor the cellular location of the presumed redox-active metals has ever been sufficiently characterized. Redox reactions of labile metals coordinated to biological macromolecules can act as catalysts for the Haber-Weiss reaction and lead to site-specific damage inflicted to critical targets. According to this mechanism, metal binding to DNA is a prerequisite for site-specific DNA damage (Goldstein & Czapski, 1986): The bound metal is reducible by reductants such as $O_2^{\bullet-}$ or ascorbate:

$$\text{DNA–L–M}^{n+} + O_2^{\bullet-} \rightarrow \text{DNA–L–M}^{(n-1)+} + O_2 \quad (4)$$

where M^{n+} denotes oxidized transition metal such as Cu^{2+} or Fe^{3+} and L represents ligand irrespective of the number of bound ligand molecules. Alternatively, the bound metal can be reduced prior to the formation of the ternary complex as was found for $(OP)_2$–copper (Thederahn et al., 1989)

$$\text{L–M}^{n+} + O_2^{\bullet-} \rightarrow \text{L–M}^{(n-1)+} + O_2 \quad (5a)$$

$$\text{DNA} + \text{L–M}^{(n-1)+} \rightleftarrows \text{DNA–L–M}^{(n-1)+} \quad (5b)$$

which in turn can react with H_2O_2 to form a peroxo complex (Rush & Koppenol, 1986; Masarwa et al., 1988)

$$\text{DNA–L–M}^{(n-1)+} + H_2O_2 \rightarrow \text{DNA–L–M}^{(n-1)+}\text{–}H_2O_2 \quad (6)$$

that can generate $^{\bullet}OH$ radicals and/or higher oxidation states of the metal (Goldstein & Czapski, 1986; Rush & Koppenol, 1986; Masarwa et al., 1988; Yamamoto & Kawanishi, 1989; Thederahn et al., 1989; Sutton & Winterbourn, 1989)

$$\text{DNA–L–M}^{(n-1)+}\text{–}H_2O_2 \rightarrow \text{DNA–L–M}^{n+} + OH^- + {}^{\bullet}OH \quad (6a)$$

$$\text{DNA–L–M}^{(n-1)+}\text{–}H_2O_2 \rightarrow \text{DNA–L–M}^{(n+1)+} + 2OH^- \quad (6b)$$

Such reactions have previously been proposed to operate in various systems, including DNA cleavage induced by $(OP)_2$–copper and H_2O_2 (Goldstein & Czapski, 1986; Rush & Koppenol, 1986; Aronovitch et al., 1987a; Masarwa et al., 1988; Yamamoto & Kawanishi, 1989; Thederahn et al., 1989).

According to this mechanism any reagent that can remove H_2O_2 (i.e., CAT), dismutate $O_2^{\bullet-}$ (i.e., SOD), bind the metals

(i.e., DFO), or successfully compete for hydroxyls (scavenger of •OH) would be anticipated to diminish the biological damage. In the present study nitroxides, in contrast to exogenously added SOD, prevented cell injury (Figure 1). Considering the SOD-like activity of nitroxides (Samuni et al., 1988) and the intracellular site of the critical damage to growing *xthA* cells, the nitroxide protective effect is attributable to removal of intracellular $O_2^{\bullet-}$ radicals. However, this explanation does not acount for nitroxide protection under hypoxic conditions. Since no superoxide radicals are expected in the hypoxic cells, our results suggest that nitroxides can contribute to cell protection also by another mechanism.

Nitroxides would protect if they could remove H_2O_2 from the system by acting as a "CAT mimic", but this possibility was excluded since the nitroxide exerted no detectable effect on H_2O_2 concentration. In addition, coordination of intracellular transition metals could modify their redox potential, reactivity, and binding site (Mitchell et al., 1989), thus affecting the biological damage. Such a presumed coordination could protect the cell by hindering metal binding to critical cellular targets. Neither, however, EPR nor spectrophotometric evidence was found for complex formation between nitroxides and copper or iron ions.

Another explanation for the nitroxides' protective effect can be found by assuming that they react with and detoxify secondary organic free radicals produced in the system. Although nitroxide free radicals are relatively stable, they rapidly combine with carbon-centered and oxygen-centered free radicals at diffusion-controlled reaction rate constants (Khloplyankina et al., 1965; Robbins & Eastman, 1970; Brownlie & Ingold, 1988). Such a mechanism for detoxification was recently proposed to decrease lipid peroxidation in cell-free systems (Takahashi et al., 1989; Nilsson et al., 1989).

Alternatively, it is possible that nitroxides compete with H_2O_2 for the reduced metal ions, either free

$$R'R\text{-}NO + H^+ + L\text{-}M^{(n-1)+} \rightarrow R'R\text{-}NOH + L\text{-}M^{n+} \quad (7)$$

or bound to the target biomolecule

$$R'R\text{-}NO + H^+ + DNA\text{-}L\text{-}M^{(n-1)+} \rightarrow R'R\text{-}NOH + DNA\text{-}L\text{-}M^{n+} \quad (7a)$$

with a consequent slowdown of reaction 6. The present results are in accord with the above mechanism, although the nature of and the critical coordination site of "redox active" cellular metals are not known. The partial cytoprotection exhibited by DFO (Aronovitch et al., 1986b), a potent iron chelator, suggests that cellular iron facilitates the damage process, as previously reported (Starke & Farber, 1985). The reaction between DNA-Fe(II) and nitroxides, previously reported (Mitchell et al., 1990) and demonstrated in Figure 6, lends further support to the assumption that R'RNO protects by preventing reaction 6.

In conclusion, the nitroxide free radicals, which are quite stable and relatively noncytotoxic, have previously been found to possess an SOD-mimetic activity. The present study suggests that nitroxides can also act through alternative mechanisms to diminish cellular damage. Presumably by oxidizing intracellular transition metals, stable five- and six-membered cyclic nitroxide free radicals protect cells against oxidative damage and prevent in vivo DNA breakage. The implications of the findings might be far reaching. Since additional nitroxides can synthetically be tailored to partition preferentially into desired cellular compartments, this class of compounds may have great potential in alleviating the many incidences of superoxide, H_2O_2, and/or metal-associated oxidative biological damage.

References

Aronovitch, J., Samuni, A., Godinger, D., Greenbaum, M., & Czapski, G. (1986a) in *Superoxide and Superoxide Dismutase in Chemistry Biology and Medicine* (Rotilio, G., Ed.) pp 343–345, Elsvier Science Publishers, London.

Aronovitch, J., Samuni, A., Godinger, D., & Czapski, G. (1986b) in *Superoxide and Superoxide Dismutase in Chemistry Biology and Medicine* (Rotilio, G., Ed.) pp 346–348, Elsvier Science Publishers, London.

Aronovitch, J., Godinger, D., Samuni, A., & Czapski, G. (1987) *Free Radical Res. Commun. 2*, 241–258.

Bailar, J. C., Jr., & Young, E. M. (1939) *Inorg. Synth. 1*, 35–38.

Belkin, S., Mehlhorn, R. J., Hideg, K., Hankovsky, O., & Packer, L. (1987) *Arch. Biochem. Biophys. 256*, 232–243.

Brownlie, I. T., & Ingold, K. U. (1967) *Can. J. Chem. 45*, 2427–2432.

Darr, D., Zarilla, K. A., & Fridovich, I. (1987) *Arch. Biochem. Biophys. 258*, 351–355.

Demple, B., Halbrook, J., & Linn, S. (1983) *J. Bacteriol. 153*, 1079–1082.

Denq, R.-Y., & Fridovich, I. (1989) *Free Radical Biol. Med. 6*, 123–129.

Goldstein, S., & Czapski, G. (1986) *J. Am. Chem. Soc. 108*, 2244–2250.

Imlay, J. A., & Linn, S. (1986) *J. Bacteriol. 166*, 519–527.

Keana, J., Keana, S., & Beetham, D. (1967) *J. Am. Chem. Soc. 89*, 3055–3056.

Khloplyankina, M. S., Buchachenko, A. L., Neiman, M. B., & Vasil'va, A. G. (1965) *Kinet. Katal. 6*, 394–943.

Lai, C. S., Froncisz, W., & Hopwood, L. E. (1988) *Biophys. J. 52*, 625–628.

Linn, S., & Imlay, J. A. (1987) *J. Cell Sci. Suppl. 6*, 289–301.

Maniatis, T., Fritsch, E. F., & Shambrook, J. (1982) *Molecular Cloning: A Laboratory Mannual*, Cold Spring Harbor Laboratory, Cold Springs Harbor, NY.

Masarwa, M., Cohen, H., Meyerstein, D., Hickman, D. L., Bakac, A., & Espenson, J. H. (1988) *J. Am. Chem. Soc. 110*, 4293–4297.

Mehlhorn, R. J., & Packer, L. (1984) *Methods Enzymol. 105*, 215–220.

Mitchell, J. B., Samuni, A., Krishna, C. M., DeGraff, W., Ahn, M. S., Samuni, U., & Russo, A. (1990) *Biochemistry 29*, 2802–2807.

Nilsson, U. A., Olsson, L.-I., Carlin, G., & Bylund-Fellenius, A.-C. (1989) *J. Biol. Chem. 264*, 11131–11135.

Rigo, A., Argese, E., Stevanato, R., Orsega, E. F., & Viglino, P. (1977) *Inorg. Chim. Acta 24*, L71.

Robbins, W. K., & Eastman, R. H. (1970) *J. Am. Chem. Soc. 92*, 6077–6079.

Rosen, G. M., Finkelstein, E., & Rauckman, E. J. (1982) *Arch. Biochem. Biophys. 215*, 367–378.

Rush, J. D., & Koppenol, W. H. (1986) *J. Biol. Chem. 261*, 6730–6733.

Sagripanti, J.-L., & Kraemer, K. H. (1989) *J. Biol. Chem. 264*, 1729–1734.

Samuni, A., Krishna, C. M., Riesz, P., Finkelstein, E., & Russo, A. (1988) *J. Biol. Chem. 263*, 17921–17924.

Samuni, A., Krishna, C. M., Riesz, P., Finkelstein, E., & Russo, A. (1989) *Free Radical Biol. Med. 6*, 141–148.

Samuni, A., Mitchell, J. B., DeGraff, W., Krishna, C. M., Samuni, U., & Russo, A. (1990) *Free Radical Res. Commun. 9*, 241–249.

Starke, P. E., & Farber, J. L. (1985) J. Biol. Chem. 260, 10099-10104.
Sutton, H. C., & Winterbourn, C. C. (1989) Free Radical Biol. Med. 6, 53-60.
Takahashi, M., Tsuchiya, J., & Niki, E. (1989) J. Am. Chem. Soc. 111, 6350-6353.
Thederahn, T. B., Kuwabara, M. D., Larsen, T. A., & Sigman, D. S. (1989) J. Am. Chem. Soc. 111, 4941-4946.
Thurman, R. G., Ley, H. G., & Scholz, R. (1972) Eur. J. Biochem. 25, 420-430.
Yamamoto, K., & Kawanishi, S. (1989) J. Biol. Chem. 264, 15435-15440.

New Insights into the Structure of A_n Tracts and B′-B′ Bends in DNA†

Vasily P. Chuprina,‡,§ Oleg Yu. Fedoroff,‡ and Brian R. Reid*,§
Research Computer Center, USSR Academy of Sciences, Pushchino, 142292 Moscow Region, USSR, and University of Washington, Seattle, Washington 98195

Received May 8, 1990; Revised Manuscript Received September 7, 1990

ABSTRACT: Energy calculations suggest that the currently available NOE distance constraints for A_n tracts in DNA are incapable of distinguishing between structures with a narrowed minor groove arising from a large propeller twist with a small inclination or from a small propeller twist with a large negative inclination. Furthermore, analysis of published data, together with energy estimations, strongly argue against bifurcated hydrogen bonding between A and T residues being the cause of the anomalous structural properties of A_n tracts. A conformational analysis of the B′-B′ junction has been performed in which a single variable base pair has been inserted between two regions of B′ structure. We have calculated low-energy structures for A_nGA_n, A_nCA_n, A_nTA_n, A_nCT_n, and T_nCA_n duplexes, where the A_n and T_n tracts were fixed in the anomalous B′ conformation. Upon optimization, all these structures were found to contain a pronounced roll-like bending into the major groove at the site of the insertion. The important factors in the formation of these B′-B′ bends are the destruction of the B′ conformation and the concomitant widening of the minor groove at the junction region in order to reduce minor groove interstrand base clashes and improve interstrand stacking energy. If the B′ conformation has strong negative inclination, the improved intrastrand stacking energy also contributes to the bending. In calculations of duplexes with A_n and T_n tracts in the B conformation instead of B′, the bending disappears.

DNA bends, discovered several years ago (Marini et al., 1982; Hagerman, 1984; Wu & Crothers, 1984; Griffith et al., 1986; Ulanovsky et al., 1986), continue to attract the attention of both theorists and experimentalists. It has been shown recently that DNA bends are implicated in several biological functions, and various possible molecular mechanisms for bending have been discussed (Trifonov, 1985; Koo et al., 1986; Diekmann, 1987; Olson et al., 1988; Hagerman, 1990; Crothers et al., 1990). One of the models that accounts for the experimental data quite well is the so-called "distributed-junction" model proposed earlier by Chuprina and Abagyan (1988a), in which bending is distributed over several base pairs. An independent model with a similar direction of bending was also proposed by Koo and Crothers (1988). The two models have much in common, though they were obtained in different ways: the Koo-Crothers model is based on gel electrophoretic data, whereas the Chuprina-Abagyan model arose largely from molecular mechanics studies. One of the important elements of the Chuprina-Abagyan model is the use of a B′-type A_n tract structure that agrees well with available NMR (Behling & Kearns, 1986; Kintanar et al., 1987; Katahira et al., 1988; Celda et al., 1989; Nadeau & Crothers, 1989) and X-ray (Alexeev et al., 1987; Coll et al., 1987; Nelson et al., 1987; Park et al., 1987; DiGabriele et al., 1989) data. This model for overall bending considers bends induced by the B-B′ junction as well as those resulting from junctions between A_n and T_n tracts, i.e., B′-B′ junctions (designated B′-B′ bends). From these calculations, the magnitude of B′-B′ bends should be significantly larger than that of B-B′ bends. Our earlier molecular mechanics studies (Chuprina & Abagyan, 1988a) also indicate that T_nA_m, A_nCGT_m, A_nGCT_m, T_nGCA_m, and T_nCGA_m sequences have a pronounced roll-like bending into the major groove in the -TTAA-, -ANNT-, and -TNNA- regions, whereas the A_nT_m sequence is unbent (or bent very little). These results provide an explanation for the dramatically different electrophoretic mobility of $[^C_GA_4T_4^G]_n$ versus $[^C_GT_4A_4^G]_n$ multimers observed by Hagerman (1986). Indeed, according to our calculations, bends should exist in the $[^C_GA_4T_4^G]_n$ multimers at both ends of the A_4T_4 region but not in the middle. However, in the $[^C_GT_4A_4^G]_n$ multimers there is an additional bend at the central junction TA that counteracts the effects of the peripheral bends, resulting in little or no overall curvature. We have also proposed (Chuprina & Abagyan, 1988a) that insertion into an A_nT_m tract of any random base pair that produces a step other than AA or AT will result in a B′-B′ bend into the major groove in the region of this insertion.

The availability of new experimental data has now prompted us to reexamine the conformational possibilities of the oligo(dA)·oligo(dT) structure. We now show that the bifurcated hydrogen bonds found in the major groove of the A_n tracts (Nelson et al., 1987) are not the main determinants of either the structural features or the anomalous properties of A_n tracts. Our conformational analysis suggests that there are still ambiguities in interpreting A_n tract NOE data in terms of helical

† Partial support from NIH Grant GM32681 to B.R.R. is gratefully acknowledged.
‡ USSR Academy of Sciences.
§ University of Washington.

0006-2960/91/0430-561$02.50/0